Optical Gain Measurements With Variable Stripe Length Technique

Article · January 2003
DOI: 10.1007/978-94-010-0149-6_21

6 authors, including:

Jan Valenta
Charles University in Prague
160 PUBLICATIONS **2,200** CITATIONS
SEE PROFILE

Kateřina Dohnalová
University of Amsterdam
42 PUBLICATIONS **1,253** CITATIONS
SEE PROFILE

Ivan Pelant
The Czech Academy of Sciences
215 PUBLICATIONS **2,651** CITATIONS
SEE PROFILE

to be published in *Towards the first silicon laser*, Ed. L. Pavesi, S. Gaponenko L. Dal Negro, NATO-ASI series, Kluwer Academic Publishers (2003)

OPTICAL GAIN MEASUREMENTS WITH VARIABLE STRIPE LENGTH TECHNIQUE

J. VALENTA[1], K. LUTEROVÁ[2], R. TOMASIUNAS[3,4], K. DOHNALOVÁ[1,2], B. HÖNERLAGE[3] and I. PELANT[2]

[1] *Charles University, Faculty of Mathematics and Physics, Ke Karlovu 3, 121 16 Praha 2, Czech Republic*
[2] *Institute of Physics, Academy of Sciences of the Czech Republic, Cukrovarnická 10, 162 53 Praha 6, Czech Republic*
[3] *IPCMS, GONLO, UMR7504, CNRS-ULP, 23 Rue du Loess, 67037 Strasbourg Cedex, France*
[4] *Institute of Materials Science and Applied Research, Vilnius University, Sauletekio 10, 2040 Vilnius, Lithuania*

The experimental method of direct optical gain G measurement in semiconductors, namely, so called the variable stripe length (VSL) method, is reviewed. At first the basic principles of the VSL technique, which may have felt into oblivion since 1971 when the method was submitted, are recalled. Description of the method in the framework of a one-dimensional kinetic model is given and a typical experimental set-up is discussed. Then some examples of application of the VSL technique in direct-gap semiconductors with high gain ($G \geq 10^2$ cm^{-1}) are presented, where interpretation of data is, as a rule, straightforward. In low-gain materials, however, several interfering effects may occur, such as the effect of transparent substrates, of the finite stripe width, the interplay of waveguiding and detection numerical aperture and a confocal effect. These phenomena are discussed and illustrated by experimental data obtained in various systems of silicon nanocrystals. A short comparison with the pump-and-probe technique is also given.

1. Introduction

Optical gain in semiconductors plays a decisive role when evaluating potential of a given semiconducting material in photonic applications: The occurrence of positive optical gain is a necessary (albeit insufficient) condition for realisation of a semiconductor laser diode. It is therefore highly desirable to have a simple and reliable experimental method enabling us to get information about the presence/absence of gain and, in affirmative case, about its magnitude. Despite the fact that semiconductor lasers are pumped by electric current, the method must be purely optical so as to circumvent possible complications arising from the necessity of fabrication of suitable electric

to be published in *Towards the first silicon laser*, Ed. L. Pavesi, S. Gaponenko L. Dal Negro, NATO-ASI series, Kluwer Academic Publishers (2003)

contacts and p-n junctions, detrimental Joule heating etc. In other words, the method should be based on optical rather than electrical pumping.

A method meeting all these requirements was proposed by Kerry L. Shaklee and co-workers from Bell Telephone Laboratories in 1971 [1,2]. The method is based on exciting a specimen of semiconductor with a laser beam focused, using a cylindrical lens, into a narrow stripe. The length of this pumped "line" is let to vary and light output (amplified spontaneous emission) is measured as a function of the stripe length *l*. This experimental technique, later on called "variable stripe length (VSL) method", became rapidly widespread and was contributing significantly to the development of a family of semiconductor lasing compounds (for instance already in 1971 (!) Shaklee et al. demonstrated high optical gain in GaN [2]). Besides such a practise-related exploitation, the VSL method was applied successfully also for studying the laws of new excitonic recombination channels in highly excited semiconductors (e.g. biexciton radiative decay and stimulated emission in CuCl [3] and exciton-exciton collisions in GaSe [4]). Later in eighties and nineties the method proved its potential also in studying low-dimensional semiconductor structures [5,6,7] and continues to be widely used to this day – not only in semiconductor optoelectronics but also for investigation of luminescence and lasing potential of e.g. polymer substances [8,9].

In the course of thirty years, however, some of the basic principles, conditions and limitations of the method seem to be lost to a considerable extent [10]. The aim of this contribution is to recall and review the fundamentals of the VSL method, to discuss its week points and application limits. In particular, we wish to turn reader's attention to possible drawbacks of the method when measuring relatively low gain values, as expected in silicon nanostructures. The article is organised as follows: In Sec. 2 the principle, experimental realisation and mathematical description of the method in terms of kinetic equations are presented. Sec. 3 reviews application of the VSL technique to the measurement of high gain in direct-gap semiconductors and displays some typical examples. Sec. 4 is devoted to potential difficulties when the method is used in low-gain materials and Sec. 5 compares briefly the VSL method with other experimental ways to measure optical gain. Sec. 6 is devoted to summary and conclusions.

2. The basis of the VSL method

Let us suppose a luminescent semiconductor sample in the form of a parallelepiped, cut or cleaved from a standard polished wafer (Fig. 1A). Photoluminescence is excited with a laser beam focused into a narrow line. In order to assure a homogeneous excitation density distribution over the whole stripe length *l*, the use of laser sources possessing a rectangular beam cross section (not a Gaussian beam) is required. An appropriate laser system from this point of view is either an excimer or N_2-laser. Fortunately, also excitation wavelengths of these lasers (308 nm in a XeCl laser or 337 nm in a N_2-laser) provide suitable high-energy photons to excite most semiconductors across the band gap. Thus these lasers appear to be almost ideal excitation sources in most cases. The use of other laser systems is, of course, not excluded (frequency doubled or tripled Nd:YAG laser etc.) but attention must be paid to guarantee a constant excitation profile along the stripe, especially when long stripes are in use.

to be published in *Towards the first silicon laser*, Ed. L. Pavesi, S. Gaponenko L. Dal Negro, NATO-ASI series, Kluwer Academic Publishers (2003)

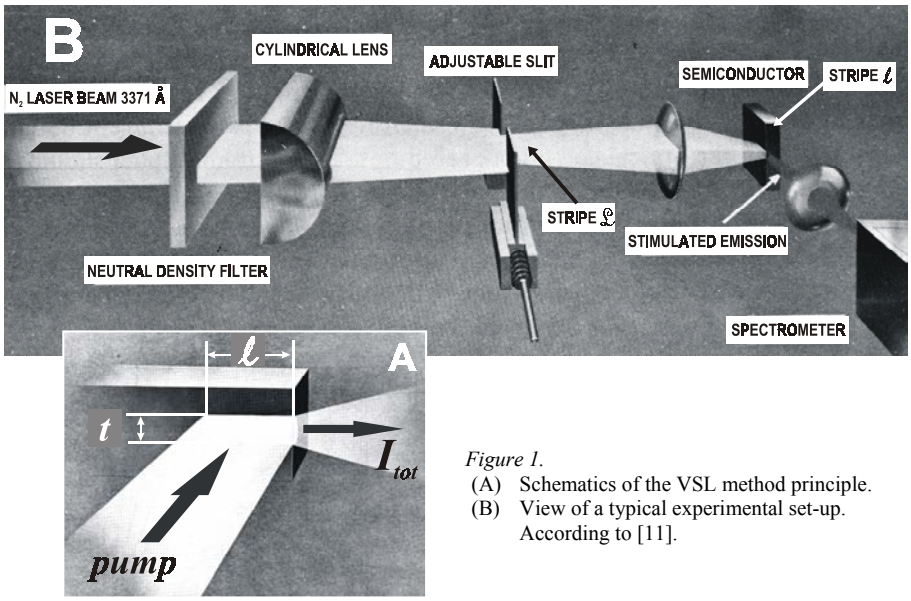

Figure 1.
(A) Schematics of the VSL method principle.
(B) View of a typical experimental set-up. According to [11].

To focus the laser beam into a stripe, the use of a cylindrical lens is obviously indispensable. Fig. 1B displays the relevant set-up in more detail [11]. As a rule, it is not the first stripe, located at the focal plane of the cylindrical lens that is projected onto the sample; this primary stripe is usually imaged by a second (spherical) lens and only this "secondary" image represents the excited region on the surface of the sample. In the focal plane of the cylindrical lens is located an adjustable slit by means of which the length of the primary image • can be varied. Such a location of the slit is dictated by the necessity of having clean cuts in the both ends of the stripe. Disadvantage may be a laser-induced damage of the slit jaws due to high excitation density but shifting the slit slightly out of the focus can prevent it.

The double projection follows two goals: First, the magnification ratio M of the spherical lens image is selected to be less than unity which increases the accuracy of determination of the stripe length $l = M.\bullet$. This is of importance especially when the investigated range of l is small, $l \leq 100$ μm. Second, the condition $M < 1$ also minimises the *unwanted effect of the diffraction pattern* that originates inevitably on the adjustable slit jaws. The stripe width t after two-lens projection usually varies between 10 μm and 20 μm. Owing to the high absorption coefficient α of semiconductors in the UV region, the penetration depth of the excitation stripe is very low, $\alpha^{-1} \cong 0.1 - 1$ μm.

Recently, we used successfully an alternative set-up (see Fig. 2): The sample was excited through a fixed metal slit (width of 10 μm or larger) placed close to the sample surface (20-50 μm). The resulting stripe length was varied by moving a metal foil over the slit with the aid of a micro-stepping motor. The signal was collected by microscope objectives (with various numerical apertures - NA), focused on the input slit of an imaging spectrograph and detected by a CCD camera [12]. This arrangement ensured the constant position of the excitation spot on the sample surface, negligible influence of

to be published in *Towards the first silicon laser*, Ed. L. Pavesi, S. Gaponenko L. Dal Negro, NATO-ASI series, Kluwer Academic Publishers (2003)

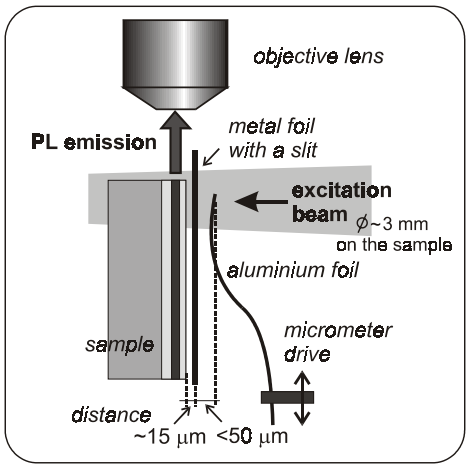

Figure 2. The set-up with a metallic slit and moving jaw close to the sample. The detection part consists of a microscope objective lens and imaging spectroscope with a CCD camera (not shown).

light diffraction (diffraction effect could be restricted to the first 10 μm of the stripe), and perfect control of the experiment geometry.

The recombination radiation originating in the excited stripe (luminescence or spontaneous emission) is emitted randomly to all directions. Spontaneous photons can induce acts of stimulated emission and this effect is monitored along the axis of the stripe by measuring the total light output intensity I_{tot} leaving the sample facet (Fig. 1A). Considering the stripe as a one-dimensional object ($l \gg t$) along the x-axis and provided population inversion is reached, the excited part of sample acts as a single-pass amplifier for photons coming in the direction of the stripe. The net gain G is defined as a relative change of light intensity passing an infinitesimal distance dx

$$G = \left[g(\lambda) - K\right] = \frac{dI(x,\lambda)}{dx}\frac{1}{I(x,\lambda)} \qquad (1)$$

where K stands for constant losses and $g(\lambda)$ is a gain coefficient (negative absorption coefficient)[#]. The total change of detected intensity when increasing stripe length by dx is a sum of a gain magnification of the incoming light and spontaneous emission $I_{sp}(\lambda)$ from the stripe of length dx:

$$dI_{tot}(x,\lambda) = \left[g(\lambda) - K\right] \cdot I_{tot}(x,\lambda) \cdot dx + I_{sp}(\lambda) \cdot dx. \qquad (2)$$

Here, it is generally accepted that $I_{sp}(\lambda)$ and $g(\lambda)$ are independent of x and, more importantly, the coupling of emission to detector is constant, independent of x.

Solving this linear inhomogeneous differential equation we retrieve the classical VSL equation [1,11]

$$I_{tot}(l,\lambda) = \exp\left[G(\lambda)\cdot l\right] \cdot I_{sp}(\lambda) \cdot \int_0^l \exp\left[-G(\lambda)\cdot x\right] \cdot dx = \frac{I_{sp}(\lambda)}{G(\lambda)}\left\{\exp\left[G(\lambda)\cdot l\right] - 1\right\} \qquad (3)$$

that enables us to evaluate net gain G from the measurement of $I_{tot}(l, \lambda)$ as a function of l. The most simple approach how to do it is to fit experiment to Eq. (3) for one or several selected wavelengths.

More complex analysis involves combination of two spectrally resolved measurements $I_{tot}(l_1, \lambda)$ and $I_{tot}(l_2, \lambda)$ at two stripe lengths l_1, l_2 (attention should be paid

[#] Note: In the language of (semiconductor) laser physics the net gain G is called cavity gain $g_C = g_{mod} - \alpha_i - \alpha_m$, where g_{mod} is a modal gain, α_i and α_m, means internal losses (inside the cavity) and mirror losses, respectively.

to be published in *Towards the first silicon laser*, Ed. L. Pavesi, S. Gaponenko L. Dal Negro, NATO-ASI series, Kluwer Academic Publishers (2003)

not to go to the stripe lengths where saturation effects appear). If $l_1 = 2l_2$ then straightforward algebra leads to an analytic expression for *gain spectrum*:

$$G(\lambda) = \left(1/l_2\right) \ln\left(\frac{I_{tot}(l_1,\lambda)}{I_{tot}(l_2,\lambda)} - 1\right). \qquad (4)$$

Let us mention that the relation (4) was used by J.M. Hvam [13] to construct a device that records directly gain spectrum by comparing signals generated with stripe lengths periodically changing between l_1 and l_2.

3. Application of the VSL technique to high-gain semiconductors

We shall demonstrate in short how the VSL technique can be applied to high gain (basically direct-gap) semiconductors. In this most simple case we may assume $G.l \gg 1$ and Eq. (3) reduces to $I_{tot}(l, \lambda) \propto \exp(G.l)$. Therefore, an exponential increase of I_{tot} with l is a direct indication of gain and the presence of stimulated emission. Fig. 3A displays one of early examples [2]: Data obtained on GaN needles at T = 2 K exhibits a linear increase of I_{tot} with l in logarithmic scale. Relevant values of G (10^3 – 10^4 cm^{-1}) can be read from the slope. At the same time this figure reveals an important feature: For longer excitation lengths l the data (full lines) deviate from the straight lines. This is due to *saturation* of the stimulated emission, a quite natural effect occurring when photon density is increased [14] because the population inversion becomes progressively exhausted and I_{tot} ultimately varies linearly with l only (gain appearing in Eq. (3) can be referred also as a small signal gain). A simple four-level model [15] predicts that a critical stripe length l_c for deviation of the experimental data from the small signal approximation (Eq. (3)) is inversely proportional to the pump intensity, $l_c \propto 1/I_{pump}$, provided G grows linearly with I_{pump}. Such behavior can be indeed found in

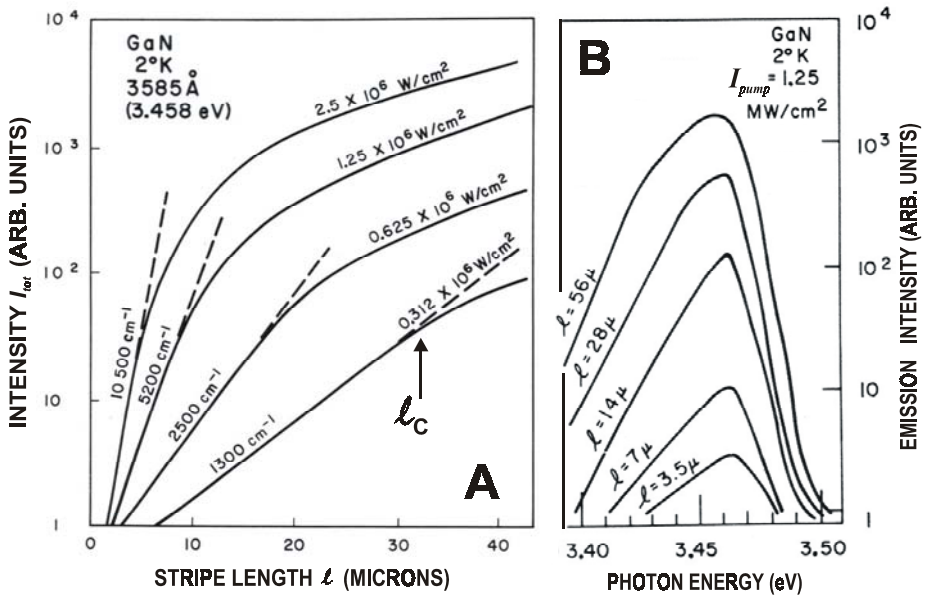

Figure 3. (A) Variation of light output from a GaN sample as a function of stripe length. Pump intensities (N_2-laser) and G values are given at each curve. (B) Evaluation of emission spectrum with increasing stripe length for pump intensity I_{pump} = 1.25 MW/cm^2. According to [2].

to be published in *Towards the first silicon laser*, Ed. L. Pavesi, S. Gaponenko L. Dal Negro, NATO-ASI series, Kluwer Academic Publishers (2003)

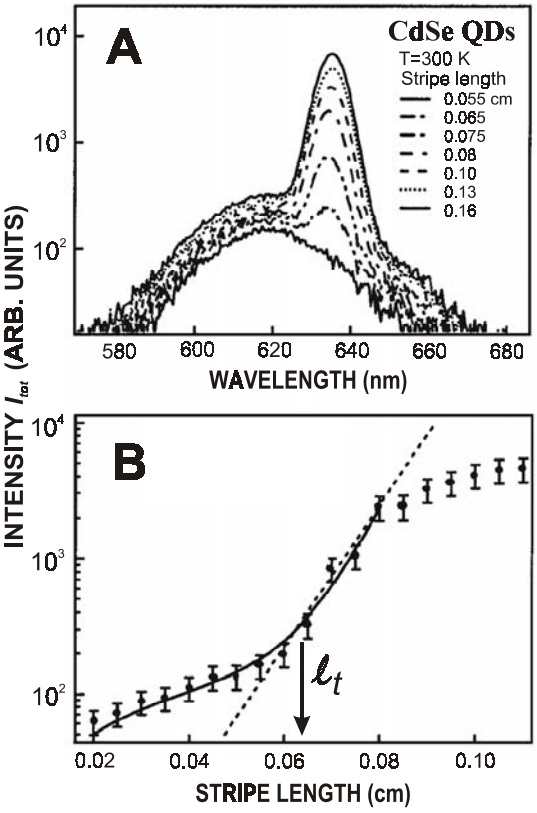

Figure 4. (A) Emission spectra of a CdSe QD film recorded using the VSL technique. (B) Data from (A) plotted as a function of the stripe length. The solid line is a fit to Eq.(5) G_{bx}=155 cm^{-1}. I_{pump} = 10 GW/cm^2, pulse duration 100 fs. A threshold stripe length l_t is indicated. According to [18].

Fig. 3A. Therefore, the appearance of a saturated region in VSL plots (like in Fig. 3A) is being generally accepted as additional evidence for stimulated emission.

In the GaN example under debate G is high, up to 10^4 cm^{-1}, i.e. its magnitude is close to the value of the optical absorption coefficient for photons with above band gap energy. One can thus interpret this particular gain as being due to band-to-band recombination of electron-hole plasma and conceive that both spontaneous and stimulated emission originate basically from identical types of excitation (homogeneous line broadening). The last claim is supported by virtually invariable emission line shape with increasing stripe length (Fig. 3B). This or similar observation (possibly a small red shift and line narrowing) justifies the use of Eq. (3) for fitting the data.

Occasionally, however, and in particular in low-dimensional systems, experiment reveals different behaviour. The exponential increase of I_{tot} occurs after exceeding a threshold stripe length l_t only and is accompanied by marked variations in the emission spectrum. A new feature in the spectrum is growing, as observed e.g. in a ZnCdSe/ZnSe quantum well [16,17] and recently in CdSe quantum dots [18] (see Fig. 4A). Possible explanation has been suggested by taking into account the existence of two types of luminescent quasiparticles (excitons and biexcitons) [18]. Emission line caused by radiative decay of biexcitons is absent in spontaneous emission because of biexciton short lifetime (fast Auger recombination in low-dimensional structures). Unlike spontaneous emission, biexcitons dominate the regime of stimulated emission and the VSL formula Eq. (3) can be rewritten as

$$I_{tot} = A_x \cdot l + \frac{A_{bx}}{G_{bx}}\left[\exp(G_{bx} \cdot l) - 1\right] \qquad (5)$$

to be published in *Towards the first silicon laser*, Ed. L. Pavesi, S. Gaponenko L. Dal Negro, NATO-ASI series, Kluwer Academic Publishers (2003)

where A_x and A_{bx} are constants proportional to spontaneous emission intensities of excitons and biexcitons, respectively, and G_{bx} is the biexciton net gain. Application of Eq. (5) enables to fit the experimental points both below and above $l_t \approx 6$ mm, see solid line in Fig. 4B, and to extract $G_{bx} = 155$ cm^{-1}.

Finally notice a trivial mathematical consequence of Eq. (3): If $(|G|.l) << 1$ then $\exp(Gl) \cong (1 + Gl)$ and thus $I_{tot}(l, \lambda) = I_{sp}(\lambda).l$. It means that in this case the monitored light emission increases *linearly* with l independently of whether $G > 0$ (true light amplification) or $G < 0$ (light attenuation along the stripe); the method is therefore hardly capable to distinguish stimulated emission from optical absorption. This indicates some problems we can encounter when studying low gain values using the VSL technique.

4. Pitfalls of the VSL method in investigation of low-gain materials

In the simple theory of the VSL method described in Section 2 there are several, more or less evident, conditions which should be fulfilled. The conditions are namely:

- *Constant excitation intensity over the whole excited stripe* (as well as homogeneity of the studied sample)
- *Negligible width of the stripe* (the theory does not account for the stimulated emission which can occur by photons going in direction other than parallel to the stripe)
- Geometrically *perfect facet of a sample*
- *Constant coupling efficiency of emission from any part of the stripe to the detector*

Some of these conditions cannot be easily met for typical samples of Si nanocrystals (Si-NCs) and similar materials. Possible problems are mainly due to:

- *Low absorption of exciting light* by Si-NCs (the concentration of Si-NCs is usually relatively low in the sample) – an important fraction of light can be reflected and refracted in the sample especially when the substrate is transparent.
- *Emitted light is guided by the sample* - the Si-NCs are often fabricated in the form of a thin layer which acts as a waveguide because of the difference in refractive indexes. Waveguiding influences significantly the coupling of emitted light to the detector optics (numerical aperture (NA) matching above all).

Now we will describe in detail several factors affecting the precision of the VSL measurement in samples with low gain.

4.1. Effect of the transparent substrate

Samples containing semiconductor quantum dots are often prepared on a transparent substrate (silica or glass slides). In this case a perfect perpendicular adjustment of the sample with respect to the pump beam must be assured, otherwise an artifact resembling to gain manifestation can be observed (Fig. 5). By opening the stripe from zero to l_1, we start to excite the luminescent film "from the back" at first (Fig. 5A), due to total internal reflection in the substrate. In this way several luminescent stripes l'_1 may

to be published in *Towards the first silicon laser*, Ed. L. Pavesi, S. Gaponenko L. Dal Negro, NATO-ASI series, Kluwer Academic Publishers (2003)

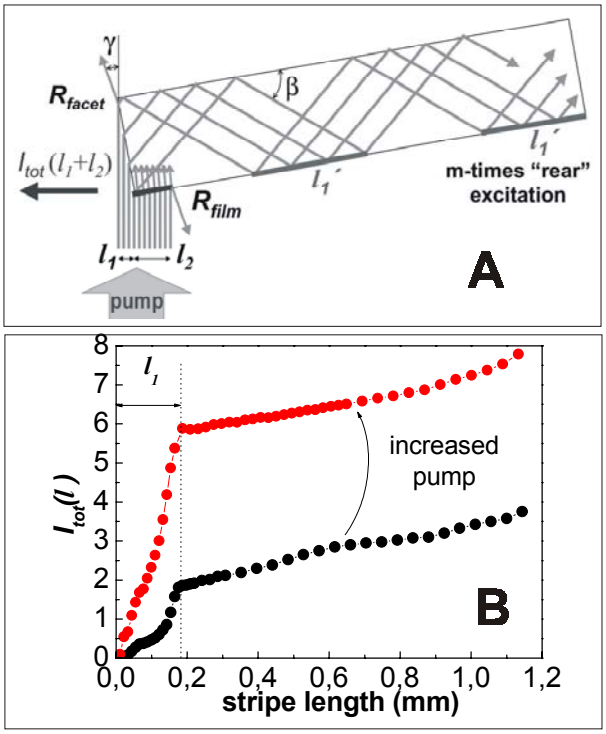

Figure 5. (A) Ray optics scheme of the VSL technique applied to a sample on a transparent substrate, whose facet is tilted by an angle γ to the pump beam. (B) Experimental demonstrations of the effect of a tilted silica substrate bearing a luminescent film without gain (γ = 10°, substrate thickness 1 mm and length 10 mm).

appear and the collecting optical system records I_{tot} growing fast with increasing l ($<l_1$). This fast growth is moreover enhanced by total internal reflection of luminescence originating in the stripes l'_1. Once the pump beam has reached the sample corner ($l > l_1$), the film is being excited from the face and further growth of I_{tot} is considerably slower since the efficient rear excitation is stopped, as well as the total internal reflection of luminescence does not apply any more. The result is shown in Fig. 5B: an abrupt break on the $I_{tot} = I_{tot}(l)$ plot, very much alike a "saturation" (however, the breaking point does not shift with varying pump intensity).

4.2. EFFECTS OF THE FINITE STRIPE WIDTH

In case of a low luminescence signal it might appear advantageous to increase the stripe width t. This can, however, entail an unwanted effect, similar to the limitation of light extraction efficiency from a planar face of a light-emitting diode (Fig. 6). Total internal reflection leads to a critical angle θ_c and a corresponding critical length

$$l'_c = t/\tan(\arcsin(1/n_{stripe})).$$

For $l \le l'_c$ only part of the emission I_{tot}

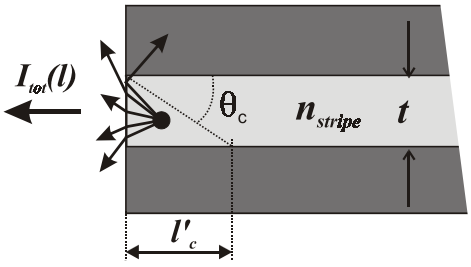

Figure 6. Limited light extraction efficiency due to total internal reflection.

to be published in *Towards the first silicon laser*, Ed. L. Pavesi, S. Gaponenko L. Dal Negro, NATO-ASI series, Kluwer Academic Publishers (2003)

can leave the sample, accordingly the plot $I_{tot} = I_{tot}(l)$ is expected to exhibit a noticeable change at l'_c, likewise that shown in Fig. 5B. For $n_{stripe} = 1.7$ and $t = 0.5$ mm we get $l'_c =$ 0,68 mm. Similar effect can be caused by a slightly oblique sample edge [19].

4.3. COUPLING OF THE EMITTED LIGHT TO A DETECTION SYSTEM

The issue of the output coupling of light emitted inside a solid-state material is important especially for fabrication of efficient light-emitting devices (see e.g. Ref. 20 and references therein) and for light-guide coupling.

In the theory of VSL technique (Section 2, Eq. (2)) there is an implicit assumption that $I_{sp}(\lambda)$ and $g(\lambda)$ are independent of x (homogeneity of the sample) and, more importantly, the *coupling of emission to detector is constant*, independent of x.

4.3.1. The shifting-excitation-spot measurement

In order to check validity of the assumption that signal from any infinitesimal part dx of the excited stripe is equally coupled to the detection system, we propose a simple modification of the VSL arrangement which we call "shifting-excitation-spot" (SES) [12] measurement. The moving shield is replaced by a moving slit perpendicular to the fixed slit (see right-hand part of Fig. 7). Consequently, only a tiny rectangular area of the sample is excited. This excited segment is moved by changing the distance x from the edge of the sample and relevant changes of detected signal are observed. If the above mentioned assumption is correct, we should observe only a slow exponential decrease of the signal (due to losses, because light amplification is precluded owing to dividing the excited stripe into small segments). With increasing distance x of the segment from the sample edge, we therefore expect:

$$dI_{SES}(x,\lambda) = I_{sp}(\lambda)\cdot\exp\left[-\left(\alpha(\lambda)+K\right)x\right]\cdot dx \qquad (6)$$

where $\alpha(\lambda)$ is a residual attenuation that is in Eqs. (1), (2) overwhelmed by gain $g(\lambda)$.

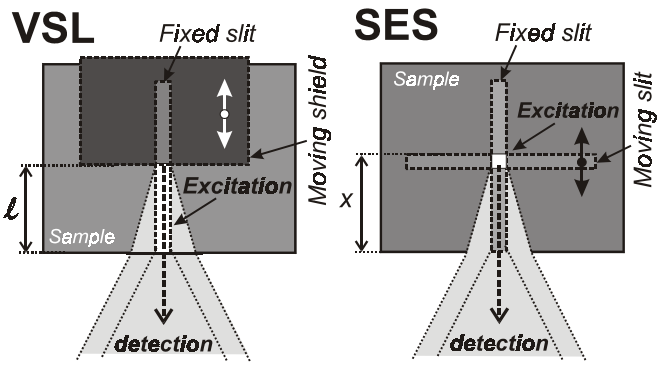

Figure 7. The modification of the VSL experimental set-up (left-hand side) for the shifted excitation spot (SES) measurements (right-hand side) [12].

For illustration we present here results of the SES measurement obtained on a sample prepared by Si-ion implantation (implantation energy of 400 keV and total dose of 4×10^{17} cm^{-2}) into a synthetic silica substrate. Annealing at 1100°C in N_2 atmosphere for 1 hour lead to formation of Si-NCs in a thin layer parallel to the silica surface [21]. Room temperature photoluminescence (PL) excited by the 325 nm line of a He-Cd laser

to be published in *Towards the first silicon laser*, Ed. L. Pavesi, S. Gaponenko L. Dal Negro, NATO-ASI series, Kluwer Academic Publishers (2003)

shows typical wide band in the red spectral region 650-900 nm [22, 23] (see Fig. 8A, curve a). This ordinary PL measurement is performed by exciting and observing the front face of the implanted plane. However, when detecting PL from the edge of the implanted layer we observe huge changes of spectral shape (Fig. 8A, curve b). The main features are the TE and TM modes guided by the nanocrystalline layer forming a planar waveguide (due to the relatively high implantation energy, the resulting layer composed of Si-NCs is buried in the SiO_2 matrix providing the refractive index contrast indispensable for waveduiding - details will be published elsewhere [24]). The modes can be distinguished using a polarizer (See Fig. 8A, curves c, d). The edges of samples were polished to a good optical quality (Fig. 8B).

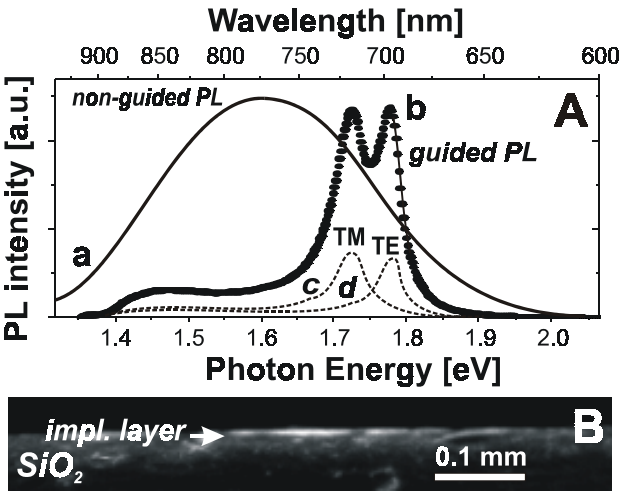

Figure 8. (A) PL spectra of a silica sample implanted with dose of 4×10^{17} cm^{-2} (λ_{exc}=325 nm and I_{exc} = 0.26 W/cm^2). Curves a and b were detected in directions perpendicular (non-guided) and parallel (guided) to the implanted plane, respectively. Dashed lines (c and d) are the polarization resolved TM and TE modes. (B) Microscope image (0.65 × 0.01 mm) of the PL emerging (in direction perpendicular to the plane of the figure) from the implanted layer. The facet of sample is slightly illuminated by a halogen lamp. According to [12].

The SES measurement at wavelengths of TE, TM modes and PL at 825 nm are plotted in Fig. 9B; the excited segment was (dx = 25 μm) × 100 μm. At the same part of the sample and under identical conditions we performed also the VSL measurement (Fig. 9A). It turns out that Eq. (6) — a *decrease* in detected light intensity with increasing x — holds for non-guided PL signal only where loss of 29 cm^{-1} was found (lower curve in Fig. 9B). Signal at TE and TM modes shows surprising *increase* for x up to about 0.5 mm. The observed dependence can be fitted, instead of Eq. (6), by a relation

$$I_{SES}(x,\lambda) = a + b \cdot x \cdot \exp[-cx]. \qquad (7)$$

There is a constant term and linear dependence on x which is prevailing for small x. For larger x the exponential decay dominates.

If there is no amplification of PL by stimulated emission, the output from the VSL measurement must give the same information as integration of the SES plot from x = 0 to l. The numerical integral of the SES measurement presented in Fig. 9B is plotted in Fig. 9C. One can see that the initial parts of curves for TE and TM modes have a superlinear shape, which can be well fitted with the VSL Eq. (3). Gain values of 29 cm^{-1} and 22 cm^{-1} were found almost identical for TE and TM modes, respectively, with the results shown in Fig. 9A. This result demonstrates that the gain-like behaviour in

to be published in *Towards the first silicon laser*, Ed. L. Pavesi, S. Gaponenko L. Dal Negro, NATO-ASI series, Kluwer Academic Publishers (2003)

Fig. 9A represents rather a consequence of a non-constant coupling of guided PL to the detection system than a true gain.

4.3.2 Interplay between output angle of guided emission and detection NA

The main reason for the observed peculiar SES dependence is the interplay between the output direction of the guided modes and the NA of detection optics (see inset in Fig. 9D). To illustrate this fact we performed the SES measurement using objectives with different numerical apertures of 0.075, 0.13, and 0.3. Results are plotted in Fig. 9D. A gradual increase of the SES signal for x up to 0.5 mm is observed with NA 0.075 and 0.13, but NA = 0.3 gives a constant signal already at $x \sim 0.1$ mm.

Therefore, our experiments demonstrate that the VSL method cannot be used in its classical form when a waveguiding effect takes place in the studied sample. In such a case, we have to consider Eq. (2) in a more general form, namely

$$dI_{tot}(x,\lambda) = \beta(x)\cdot[g(\lambda) - K]\cdot I_{tot}(x,\lambda)\cdot dx + \beta(x)\cdot I_{sp}(\lambda)\cdot dx. \qquad (8)$$

Here we introduce a coupling function $\beta(x)$. The general integral of this differential equation is:

$$I_{tot}(x) = \exp\left[G(\lambda)\cdot\int\beta(x)\cdot dx\right]\cdot I_{sp}\int\beta(x)\cdot\exp\left[-G(\lambda)\cdot\int\beta(x)\cdot dx\right]\cdot dx. \qquad (9)$$

When $\beta(x)$ is constant we retrieve the classical VSL Eq. (3). The coupling function $\beta(x)$ can be determined from the SES measurement that obviously yields

$$I_{SES}(x,\lambda) = I_{sp}(\lambda)\cdot\exp[-(\alpha(\lambda)+K)x]\cdot\beta(x)\cdot dx. \qquad (10)$$

By performing the VSL and the SES measurement under otherwise identical condition we can check if the SES signal $I_{SES}(x,\lambda)$ increases with x and whether a complicated coupling of PL signal to the detection takes place. Then either the experimental condition should be modified (with aim to have $\beta(x)$ constant) or the function $\beta(x)$ has to be determined from the SES measurement (by comparing Eqs. (7) and (10)) and solving Eq. (9) (numerically) to find $G(\lambda)$. For our samples the real net optical gain $G(\lambda)$ turns to be close to zero under excitation by a cw laser, λ_{exc}=325 nm and a pump intensity up to 1 W/cm^2.

Another example of combining the VSL and SES measurements in silicon quantum dots is shown in Fig. 10. The investigated sample is schematically displayed in Fig. 10(a). It consists of a layer of highly concentrated Si-NCs embedded in a SiO_2 matrix. The sample was prepared in the following way. At first, p-type c-Si wafer $\rho \sim$ 0.1 Ωcm was etched in a solution composed of 6 volumes of 50 wt. % HF and 15 volumes of added ethanol (14.3 % HF concentration). The etching current density was kept relatively low (1.6 mA/cm^2) so as to achieve prolonged etch time leading to higher porosity and, consequently, low mean size of Si-NCs and blue shifting of the photoluminescence band [25]. Spontaneous luminescence spectrum of resulting porous silicon (por-Si) was peaked at ~680 nm. (This particular approach was chosen to maximize the contribution of phononless radiative transitions inside Si-NCs [26] and

to be published in *Towards the first silicon laser*, Ed. L. Pavesi, S. Gaponenko L. Dal Negro, NATO-ASI series, Kluwer Academic Publishers (2003)

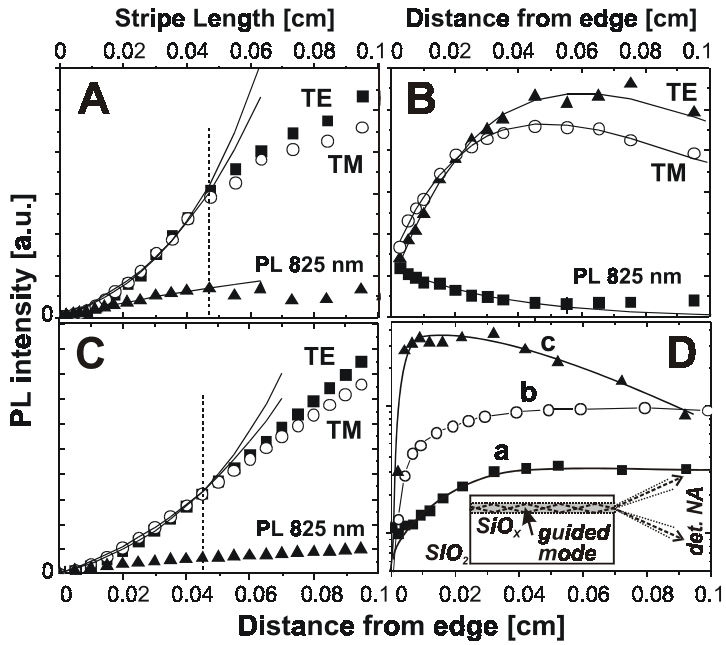

Figure 9. (A) Results of the VSL measurement at the peak of TE and TM mode and for non-guided PL around 825 nm. The fits (lines) with Eq. (3) give values of G = 35 cm^{-1} and 28 cm^{-1} for TE and TM modes, respectively, and losses of 11 cm^{-1} for non-guided PL. (B) Results of the SES measurement performed under identical conditions as the VSL. The lines are fits using Eqs. (7) and (6) for TE (TM) and PL, respectively. (C) Integration of data from panel (B). The gain fits (lines), when using formally again Eq. (3), give values of G = 29 cm^{-1} and 22 cm^{-1} for TE and TM modes, respectively. (D) The SES measurements using the detection NA of 0.075 (*a* - black squares), 0.13 (*b* - white dots), and 0.3 (*c* - black triangles). Lines are guides to the eye. The inset shows interplay between the exit angle of the guided mode and the detection NA. According to [12].

thus to increase the chance of stimulated emission to overcome losses due to the free carrier absorption [27].)

The por-Si layer was then mechanically scratched and dispersed in spin-on-glass P507 sol with the initial concentration of 1mg/200 µl. After 15 min treatment in an ultrasonic bath the suspension was let to solidify in a glass cuvette 1x1 cm^2 at 40 ^{o}C for 6 days. During solidification the por-Si powder was sedimenting to the bottom of the cuvette which resulted into creation of a brightly luminescent film of close-packed Si-NCs. Thickness of the film (measured by using fluorescence microscope image) was 62 µm which yields mean nanocrystal concentration of about 1.10^{18} NCs/cm^3.

The described transformation of a por-Si layer into a film of close-packed Si-NCs in a transparent SiO_2 matrix had three aims in view: (i) Achieving of a higher concentration of Si-NCs, (ii) avoiding excess heating of the nanocrystals since the non-absorbed excitation power propagates basically unattenuated through the matrix and (iii) an additional blue shifting and emission intensity enhancement due to phosphorus [28,29] contained in P507 spin-on-glass. In the outlook for the future, such a close-packed system of nanocrystals should also assure better transport properties than native por-Si or layers prepared by standard Si^+-implantation.

to be published in *Towards the first silicon laser*, Ed. L. Pavesi, S. Gaponenko L. Dal Negro, NATO-ASI series, Kluwer Academic Publishers (2003)

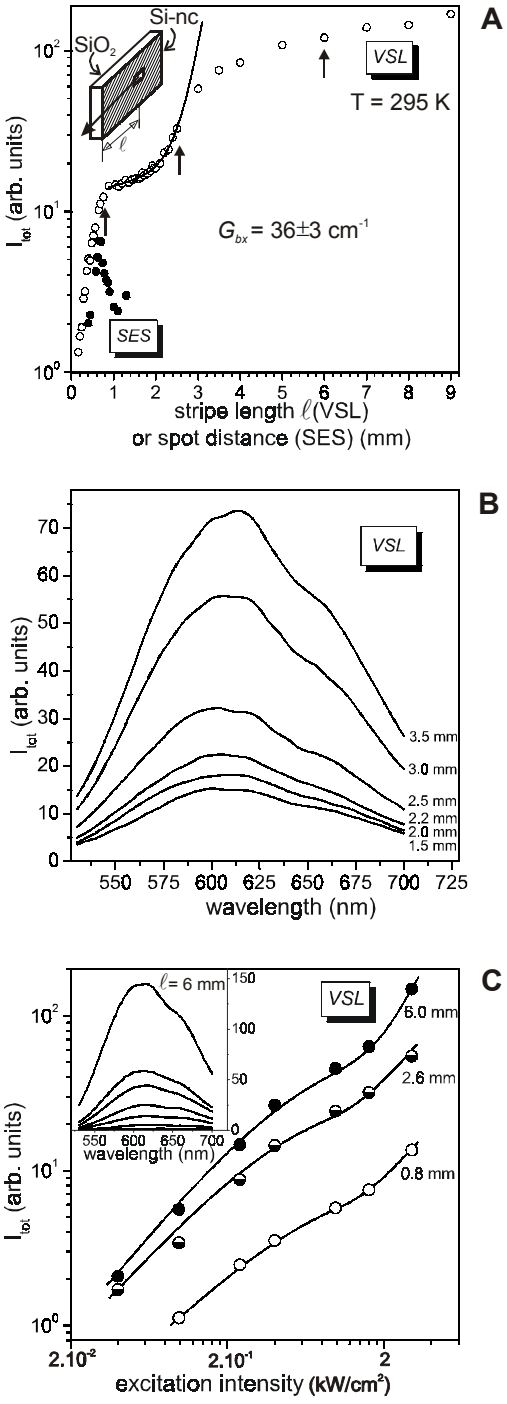

Once solidified, the sample was turned out of the cuvette and used as a free-standing layer for VSL and SES measurements. Photoexcitation was provided with a XeCl excimer laser (308 nm, 18 ns) at room temperature.

Room temperature experimental data obtained by using the both methods is displayed in Fig. 10A. There are two interesting features worth discussing. First, the VSL measurement (o) starts up with an initial exponential part up to $l_o \cong$ 0.8 mm followed by a linear section resembling to a "saturation". The SES data points (•) start also with a nonlinear growth terminating at the same l_o but an abrupt decrease follows for $l > l_o$. Such a behavior is similar to that found in the Si^+-implanted SiO_2 sample with pronounced waveguiding effects as discussed above (Fig. 9A, B). We interpret therefore this observation as the aperture effect of the collecting lens and conclude that the initial exponential part in the VSL measurements is not due to a real gain.

The second interesting feature in Fig. 10A is the second growth in VSL data for l above approx. 2 mm, followed again by a saturation-like region. The appearance of such a "threshold" stripe length resembles

Figure 10. (A) Room-temperature VSL (○) and SES (●) data taken on a long sample of Si-NCs prepared by etching of crystalline Si (see text). The solid line is a fit to Eq. (5) with G_{bx} = 36 cm^{-1}. Pump intensity ~3 kW/cm^2, 308 nm, 18 ns. (B) Emission spectra corresponding to (a), measured at several different stripe lengths. (C) Light output I_{tot} as a function of pump intensity at three different stripe lengths (indicated by arrows in A). The lines are guides for the eye. Inset: Evolution of the emission spectrum with pump intensity for l = 6 mm.

to be published in *Towards the first silicon laser*, Ed. L. Pavesi, S. Gaponenko L. Dal Negro, NATO-ASI series, Kluwer Academic Publishers (2003)

strongly to the results reported recently by Malko et al. in CdSe nanoparticles [18] and interpreted in terms of biexciton gain, see Fig. 4B. Applying Eq. (5) with an appropriate background to the VSL data in Fig. 10A we obtain a good fit (solid line) and a reasonable value of gain G_{bx} =36 cm^{-1}. Moreover, the onset of the saturation-like region ($l \geq 2.8$ mm) is observed for $Gl \approx 10$, i.e. for the same value of the Gl product like in other low-dimensional systems exhibiting unambiguous gain! [16,18] It is thus very tempting to interpret the second increase in I_{tot} here as owing to the presence of real gain. However, two additional observations are against this interpretation: Emission spectra taken at several l between 1.5 and 3.5 mm (shown in Fig. 10B) exhibit no indication of a new developing spectral feature. More importantly, the variation of the light output I_{tot} as a function of excitation intensity, displayed in Fig. 10C, shows very similar behavior for three fixed excitation lengths (l = 0.8 mm, 2.6 mm and 6 mm) without any significant break to superlinear increase. We thus feel that not even in case of this especially prepared long sample with Si-NCs experiment can bring conclusive evidence for optical gain.

These experiments thus demonstrate that the efficient waveguiding, which is desirable for more efficient amplification of spontaneous emission, may cause substantial problems in application of classical VSL technique. Possible solutions are outlined in Section 6.

4.3.3 Confocal effect in the detection of the VSL signal

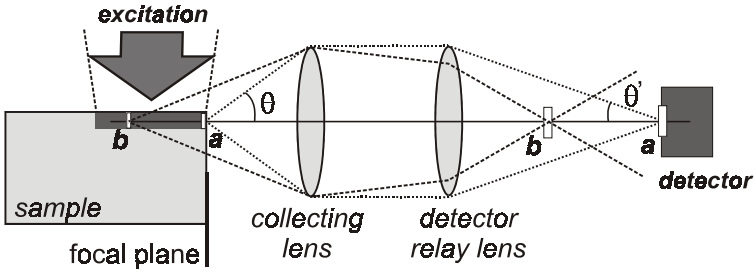

Figure 11. The basic principle of the confocal effect.

Another effect, which could contribute to the non-constant coupling efficiency of light coming from different points of a sample, can be called the confocal effect.

The common arrangement for collection and detection of emitted light in luminescence spectroscopy is an imaging of the emitting spot located on the sample facet (point *a* in Fig. 11) to the detector (or the input slit of the spectrometer). High NA and short focus collecting lens is preferred in order to have a good efficiency of light collection, while the relay lens is usually of longer focus (in order to match the spectrometer NA). Therefore the image is usually magnified in the detection plane. In the measurement of a weak gain with the VSL method a long excited stripe is sometimes used. In such a case the emitting points of the sample which are far from the output facet (point *b* in Fig. 11) will be imaged in a plane in front of the detector. Then, if the detector size is small (or the input spectrometer slit is narrow) some light will be lost around the detector. The effect will be stronger when the collecting lens NA is higher (i.e. the depth of focus is smaller), magnification of the optical system is higher and the detector size smaller.

to be published in *Towards the first silicon laser*, Ed. L. Pavesi, S. Gaponenko L. Dal Negro, NATO-ASI series, Kluwer Academic Publishers (2003)

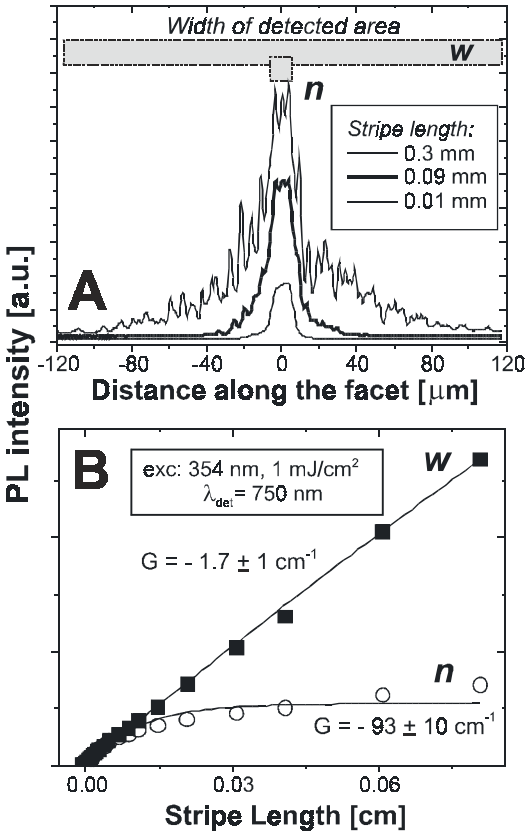

Figure 12. Illustration of the confocal effect: VSL measurement with a high NA_{det}=0.45, when either all signal coming from the sample facet (240 μm wide area) or just a signal from the area corresponding to the image of the excited stripe (10 μm) is detected. (A) PL intensity profiles of the output facet (illustration of defocusing of emission from points distant from the edge), (B) the VSL stripe dependence for the two widths of detection area.

In fact this is the same effect as that used in confocal microscopes to achieve depth resolution so we can use theory developed for confocal microscopes [30]. The VSL experiment corresponds to the observation of fluorescence plane reflectors with pinhole or slit detector in confocal microscope. For emitters far from the focus the detected intensity should decrease as $1/z^2$ or $1/z$ for pinhole and slit detector, respectively [30].

To illustrate the confocal effect we show in Fig. 12 VSL measurements on Si-ion implanted silica layers using an objective lens with NA = 0.45. The CCD images show that for long stripes the emitting spot becomes significantly larger. Restriction of the detection area in the image plane from 240 μm (which covers all the signal, area *w* in Fig. 12A) to a narrow area *n* of about 10 μm (corresponding to the width of excited stripe) causes significant loss of signal, which is observed as increased losses (93 instead of 1.7 cm^{-1}).

It should be quite easy to avoid the confocal effect using low NA optics (contrary to call for high NA dictated by efficient coupling of guided light – Section 4.3.2) and a large-area detector (spectrometer slit). In addition the effect can be identified and corrected using the SES measurement.

5. Comparison of the VSL technique with other methods of gain measurement

5.1. Detection of absorption changes by the pump-and-probe technique

Because optical gain is defined as negative absorption, the most straightforward technique to measure it consists in the detection of absorption changes when pumping a

to be published in *Towards the first silicon laser*, Ed. L. Pavesi, S. Gaponenko L. Dal Negro, NATO-ASI series, Kluwer Academic Publishers (2003)

sample to the population inversion. In other words, this is a *pump-and-probe technique* (P&P) in which optical absorption in a sample spot excited with a strong pumping (laser) beam is tested by a weak probe beam.

The *P&P technique in transmission geometry* (we do not discuss the possibility to calculate absorption changes from reflection measurement) has several limitations. First of all, the sample should be self-supporting or lay on a substrate that is transparent at the investigated range of wavelengths. The thickness of the sample d is limited by the necessity to achieve a perfect spatial overlap of the pumping and probing beams through the whole excited volume (let us estimate the upper limit to be d = 1 mm). *At the pumping wavelength the sample has to be optically thin*, i.e. the absorption coefficient α of the material under study must be low enough to allow penetration of the exciting beam through the sample and creation of a relatively homogeneous photocarrier population (if a 10% decrease of excited light is allowed, we obtain αd = -ln(0.9) = 0.105, hence for $\alpha = 10^3$ cm^{-1} d is limited to 1 μm). (Note: Attention should be paid also to a *possible lensing effect* – the test beam may be focused/defocused and/or deflected by the dynamic lens created by the induced refraction index changes in the excitation spot [31].)

The smallest detectable absorption (gain) changes $\Delta\alpha$ are determined by the dynamic range of the detection system (i.e. the ratio of a maximum detectable signal S_{max} to the detector noise level N_{det}, which can reach 10^4-10^5 in good systems) and by the shot noise (it is equal to square root of the detected signal $(S)^{1/2}$, typically 1%, but its influence can be effectively reduced in some cases by a numerical treatment – smoothing). In other words, the relative induced changes of the transmitted signal should be equal or greater than the reciprocal "effective" dynamic range r (including shot noise and signal treatment):

$$\frac{I_0 \exp[-(\alpha+\Delta\alpha)d] - I_0 \exp(-\alpha d)}{I_0 \exp(-\alpha d)} \geq \frac{N_{det} + \sqrt{S}}{S_{max}} = r^{-1}. \qquad (11)$$

Here I_0 is input test beam intensity and α is the sample absorption coefficient without pumping. After simple operations we found (for $r >> 1$):

$$\Delta\alpha d \geq \ln(1 + 1/r) \cong 1/r. \qquad (12)$$

For a system with the effective dynamic range of 10^3 we get $\Delta\alpha.d \geq 10^{-3}$. For a typical sample of Si-NCs in a SiO_2 matrix with $d \sim 0.5$ μm we need $\Delta\alpha = G \geq 20$ cm^{-1}, therefore the P&P technique seems not to be suitable for such low-gain samples.

The VSL method is in principle also a kind of P&P technique where spontaneous emission itself plays a role of the test beam. Therefore, the method is applicable for those wavelengths only where spontaneous emission is strong enough. The advantage of the VSL technique is a simpler experimental arrangement with just one laser beam (and, moreover, principal acceptance of non-transparent substrates). The lower limit for the $G.l$ product should be basically the same as given by Eq. (12) but the specific features of the VSL technique (Section 3) set this limit to $G.l \cong 1$. There is also an upper limit that stems from two facts. First, exponential VSL section saturates generally [32] for $G.l_C \sim 5$ (see e.g. Fig. 3A). Second, inevitable pump light diffraction prevents exciting homogeneously stripes shorter than about 10 μm. Thus high gains which produce saturation of the VSL signal within l~10 μm, i.e. $G \geq 5 \times 10^3$ cm^{-1}, turn to be

to be published in *Towards the first silicon laser*, Ed. L. Pavesi, S. Gaponenko L. Dal Negro, NATO-ASI series, Kluwer Academic Publishers (2003)

measurable with difficulty. Such high gains, however, occur only exceptionally (e.g. in GaN). All these considerations are summarised in Tab. I.

TABLE I. Estimation of limits for application of the VSL and P&P techniques

Method	lower limit	upper limit	notes
P&P	$Gd \geq 10^{-3}$	___	$\alpha(\lambda_{pump})d \leq 0.1$ $d \leq 1$ mm
VSL	$Gl \geq 1$	$G \leq 5 \times 10^3$ cm^{-1}	

Taking into account that the stripe length l can be as much as by four orders of magnitude larger that a typical film thickness d, we may conclude that the P&P technique is good for high-gain materials while the VSL method is better suited for the small gains. The applicability of both methods is, of course, very sensitive to optical and geometrical properties of studied samples. In some cases it is possible to apply both techniques and compare them. In Fig. 13 we show results of gain measurement by both the VSL and P&P methods in CuBr-NCs embedded in a glass plate (thickness ~0.4 mm). The net gain of about 10 cm^{-1} is interpreted to be due to trapped biexcitons [33].

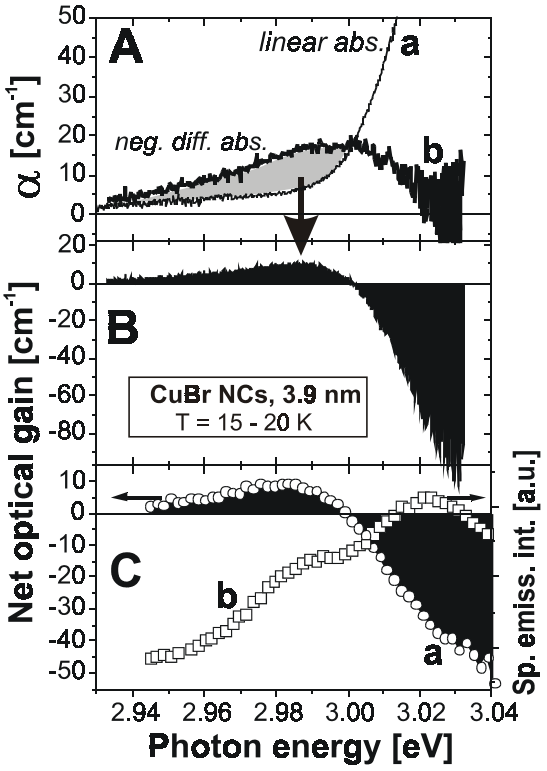

Figure 13. Comparison of the P&P and VSL techniques for measurement of gain in CuBr-NCs (mean radius 3.9 nm, T=15-20 K).
(A) Linear absorption at the edge of excitonic band (a) compared with the negative differential absorption (b) produced by band-to-band excitation at 308 nm (150 kW/cm^2).
(B) (B) Net optical gain is a difference between curves *a* and *b* in (A).
(C) Spectra of net gain (a) and spontaneous emission (b) calculated from VSL measurements (excitation at 308 nm, 110 kW/cm^2).
According to [33].

5.2. OPTICAL GAIN MEASUREMENT WITH ELECTRICAL PUMPING

The above-mentioned P&P and VSL techniques are optimal for testing gain potential of a given semiconductor material. The second step towards a semiconductor laser device is, however, an electrically pumped gain measurement. There are several techniques of

to be published in *Towards the first silicon laser*, Ed. L. Pavesi, S. Gaponenko L. Dal Negro, NATO-ASI series, Kluwer Academic Publishers (2003)

this type. One of them is the analogue of the VSL technique, sometimes called *optical stripe length method* (OSLM), where several segments of a stripe-like contact excite electroluminescence starting from the edge of a sample [34]. The Henry method [35] calculates gain from the device spontaneous emission spectra (below the laser threshold). The method is not generally applicable since knowledge of the carrier distribution function is required. The Hakki-Paoli [36] method deduces the gain from the contrast of Fabry-Perot oscillations below the threshold, so a good cavity is necessary as well as a good spectral resolution.

6. Conclusions

The VSL method is suitable for gain measurements from $G.l \cong 1$ to $G \leq 5 \times 10^3$ cm^{-1}. The technique looks very simple and is tempting to underestimate systematical experimental errors. However, there is quite a lot of "snags" that one has to be aware of. Attempting to emphasize the best laboratory practice for the VSL method, we can say: *Check exact adjustment of the experiment, make the excited stripe as narrow as possible, combine the VSL and SES measurements under identical conditions, try to modify the experimental conditions until the SES results follows Eq. (6).* There seems to be one simpler alternative how to avoid the "coupling" and edge-related problems: To perform the VSL measurements inside the sample, i.e. to start the excited stripe not at the facet but at a certain distance from the edge (Fig. 14A) [37]. The very best experiment would be to couple a weak spectrally broad light beam into the waveguide and look for absorption/gain changes during optical pumping (pump-and-probe experiment under the same conditions as the VSL, Fig. 14B).

Finally, it should be kept in mind that the exponential shape of the VSL curve, followed by a saturation region, is not sufficient to prove the presence of gain. Investigating emission spectral changes should complete this observation, along with variation of the emission intensity as a function of pump intensity (break in the slope) and time resolved studies (pulse shortening).

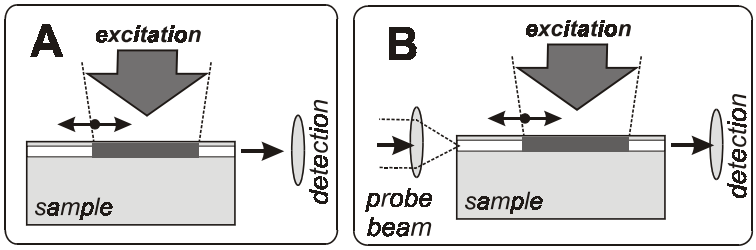

Figure 14. (A) Alternative VSL measurement inside the sample, (B) P&P experiment under the same conditions with a probe beam coupled to the waveguide.

to be published in *Towards the first silicon laser*, Ed. L. Pavesi, S. Gaponenko L. Dal Negro, NATO-ASI series, Kluwer Academic Publishers (2003)

Acknowledgement

This work was supported by the projects A1010809 and AVOZ 1010914 of GAAVCR, the project 202/01/D030 of GACR, by the NATO (PST.CLG.978100) and by the Royal Swedish Academy of Sciences. One of us (R.T.) appreciates the financial support from the Lithuanian State Foundation for Science and Studies. We are grateful to Prof. J. Linnros for stimulated discussions, to Dr. S. Cheylan for fabrication of high quality samples and to Dr. A. Galeckas, Dr. P. Gilliot and Dr. O. Crégut for experimental assistance.

References

1. Shaklee, K.L. and Leheny, R.F. (1971) Direct observation of optical gain in semiconductors, *Appl. Phys. Letters* **18**, 475-477.
2. Dingle, R., Shaklee, K.L., Leheny, R.F. and Zetterstrom, R.B. (1971) Stimulated emission and laser action in Gallium Nitride, *Appl. Phys. Letters* **19**, 5-7.
3. Shaklee, K.L., Leheny, R.F. and Nahory, R.E. (1971) Stimulated emission from the excitonic molecules in CuCl, *Phys. Rev. Letters* **26,** 888-891.
4. Capozzi, V. and Staehli, J.L. (1983) Spontaneous and optically amplified luminescence from exciton-exciton collisions in GaSe at liquid-He temperature, *Phys. Rev.* **B28,** 4461-4467.
5. Bylsma, R.B., Becker, W.M. Bonsett, T.C., Kolodziejski, L.A., Gunshor, R.L., Yamanashi, M. and Datta, S. (1985) Stimulated emission and laser oscillations in ZnSe-$Zn_{1-x}Mn_xSe$ multiple quantum wells at ~453 nm, *Appl. Phys. Letters* **47,** 1039-1041.
6. Gutowski, J., Diesel, A., Neukirch, U., Weckendrup, D., Behr, T., Jobst, B. and Hommel, D. (1995) Exciton dynamics and gain mechanismsms in optically pumped ZnSe-based laser structures, *phys. stat. sol. (b)* **187,** 423-434.
7. Butty, J., Peyghambarian, N., Kao, Y.A. and Mackenzie, J.D. (1996) Room temperature optical gain in sol-gel derived CdS quantum dots, *Appl. Phys. Letters* **69,** 3224-3226.
8. McGehee, M.D., Gupta, R., Veenstra, S., Miller, E.K., Díaz-García, M.A. and Heeger, A.J. (1998-I) Amplified spontaneous emission from photopumped films of a conjugated polymer, *Phys. Rev.* **B58,** 7035-7039.
9. Díaz-García, M.A., De Ávilla, S.F. and Kuzyk, M.G. (2002) Dye-doped polymers for blue organic diode lasers, *Appl. Phys. Letters* **80,** 4486-4488.
10. It is interesting to note that the references 1, 3 and 11 have been cited according to Science Citation Index (since 1980) almost 400 times but in many articles nowadays the VSL technique is applied even without citing the original papers.
11. Shaklee, K.L., Nahory, R.E. and Leheny, R.F. (1973) Optical gain in semiconductors, *J. Luminescence* **7,** 284-309.
12. Valenta, J., Pelant, I. and Linnros, J. (2002) Waveguiding effects in the measurement of optical gain in a layer Si nanocrystals, *Appl. Phys. Letters*, **81**, 1396-1398.
13. Hvam, J.M. (1978) Direct recording of optical-gain spectra from ZnO, *J. Appl. Phys*. **49**, 3124-3126.
14. Saleh, B.A.E. and Teich, M.A. (1991) *Fundamentals of Photonics*, J. Wiley & Sons, New York.
15. Shaklee, K. L., Nahory, R.E. and Leheny, R.F. (1972) Stimulated recombination highly excited semiconductors, in *Proc. 11th Int. Conf. Phys. Semicond. , Warszava 1972, Vol. 2*, Polish Scientific Publishers, Warszawa, pp. 853-862.
16. Tomasiunas, R., Pelant, I., Hönerlage, B., Lévy, R., Cloitre, T. and Aulombard, R.L. (1998-II) Stimulated emission and optical gain in a single MOVPE-grown ZnCdSe-ZnSe quantum well, *Phys. Rev*. **B57,** 13077-13085.
17. Mikulskas, I., Luterová, K., Tomasiunas, R., Hönerlage, B., Cloitre, T. and Aulomard, R.L. (1998) Light amplification due to free and localized exciton states in ZnCd Se GRINSCH structures, *Appl. Phys.* **A67**, 121-124.
18. Malko, A.V., Mikhailovsky, A.A., Petruska, M.A., Hollingsworth, J.A., Htoon, H., Bawendi, M.G. and Klimov, V.I. (2002) From amplified spontaneous emission to microring lasing using nanocrystal quantum dot solids, *Appl. Phys. Letters* **81,** 1303-1305.

to be published in *Towards the first silicon laser*, Ed. L. Pavesi, S. Gaponenko L. Dal Negro, NATO-ASI series, Kluwer Academic Publishers (2003)

19. Mohs, G., Aoki, T., Shimano, R., Kuwata-Gonokami, M. and Nakamura, S. (1998) On the gain mechanism in GaN based diodes, *Solid State Com.* **108**, 105-109.
20. Benisty, H. (1999) Physics of light extraction efficiency in planar microcavity light-emitting diodes, in H. Benisty, J.-M. Gérard, R. Houdré, J. Rarity and C. Weisbuch (eds.), *Confined Photon Systems*, Springer-Verlag, Berlin, pp. 393-405.
21. Elliman, R.G., Lederer, M.J. and Luther-Davis, B. (2002) Optical absorption measurements of silica containing Si nanocrystals produced by ion implantation and thermal annealing, *Appl. Phys. Letters.* **80**, 1325-1327.
22. Guha, S. (1998) Characterization of Si^+ ion-implanted SiO_2 films and silica glasses, *J. Appl. Phys.* **84**, 5210-5217.
23. Linnros, J., Lalic, N., Galeckas, A. and Grivickas, V. (1999) Analysis of the stretched exponential photoluminescence decay from nanometer-sized silicon crystals in SiO_2, *J. Appl. Phys.* **86,** 6128-6134.
24. Valenta, J., Pelant, I., Luterová, K., Tomasiunas, R., Cheylan, S., Elliman, R.G., Linnros, J. and Hönerlage, B., An active planar optical waveguide made from luminescent silicon nanocrystals, submitted to *Appl. Phys. Letters.*
25. Canham, L.T. (1990) Silicon quantum wire array fabrication by electrochemical and chemical dissolution of wafers, *Appl. Phys. Letters* **57,** 1046-1048.
26. Hybertsen, M.S. (1994) Absorption and emission of light in nanoscale silicon structures, *Phys. Rev. Letters.* **72,** 1514-1517.
27. Dumke, W.P. (1962) Interband transitions and laser action, *Phys. Rev.* **127,** 1559-1563.
28. Fujii, M., Mimura, A., Hayashi, S. and Yamamoto, K. (1999) Photoluminescence from Si nanocrystals dispersed in phosphosilicate glass thin films: Improvement of photoluminescence intensity, *Appl. Phys. Letters.* **75,** 184-186.
29. Mimura, A., Fujii, M., Hayashi, S., Kovalev, D. and Koch, F. (2000) Photoluminescence and free-electron absorption in heavily phosphorus-doped Si nanocrystals, *Phys. Rev.* **B62** 12625-12627.
30. Corle, T.R. and Kino, G.S. (1996) *Confocal Scanning Optical Microscopy and Related Imaging Systems*, Academic Press, New York.
31. Klingshirn, C. (1995) *Semiconductor Optics*, Springer-Verlag, Berlin.
32. Klingshirn, C. and Haug, H. (1981) Optical properties of highly excited direct gap semiconductors, *Phys. Reports* **70**, 315-398.
33 Valenta, J., Dian, J., Gilliot, P. and Hönerlage, B. (2001) Photoluminescence and optical gain in CuBr semiconductor nanocrystals, *phys. stat. sol*. (b) **224**, 313-317.
34. Bognár, S., Grundmann, M., Stier, O., Ouyang, D., Ribbat, C., Heitz, R., Sellin, R., and Bimberg, D. (2001) Local modal gain of InAs/GaAs quantum dot lasers, *phys. stat. sol. (b)* **224,** 823-826.
35. Henry, C.H., Logan, R.A. and Merritt, F.R. (1980) Measurement of gain and absorption spectra in AlGaA buried heterostructure lasers, *J. Appl. Phys*. **51,** 3042-3050.
36. Hakki, B.W. and Paoli, T.L. (1975) Gain spectra in GaAs double-heterostructure injection lasers, *J. Appl. Phys.* **46,** 1299-1306.
37. We thank to Dr. L. Khriachtchev for suggesting us this idea.